

THIS IS A PREPRINT VERSION OF THE ARTICLE:

Energy loss of MeV protons in diamond: Stopping power and mean ionization energy

FULL VERSION HAS BEEN PUBLISHED IN THE “Diamond & Related Materials” and is available online at:

<https://doi.org/10.1016/j.diamond.2022.109621>

Energy loss of MeV protons in diamond: stopping power and mean ionization energy

Andrej Crnjac¹, Milko Jakšić¹, Matija Matijević¹, Mauricio Rodriguez-Ramos¹, Michal Pomorski², and Zdravko Siketić¹

¹Division of Experimental Physics, Ruđer Bošković Institute, 10000 Zagreb, Croatia

²Université Paris-Saclay, CEA, List, F-91120 Palaiseau, France

Sažetak

The energy loss of protons, in the range between 1.6 MeV and 6 MeV, in a 3.5 μm thick single-crystal diamond membrane was determined by the transmission method. The thickness and surface uniformity of the target were checked by two independent techniques before ion beam irradiation. The stopping power of diamond was evaluated from these data and compared with SRIM Monte Carlo simulations of ion transport, showing a slight overestimate of the simulated values over the experimental stopping powers. In addition, a comparison was made with theoretical calculations based on the Bethe formula to extract the mean ionization potential, I , of carbon atoms in diamond. The obtained I -value was $81 \pm 4 \text{ eV}$. A discussion and comparison with results of other authors is given.

Keywords: diamond membrane, ion beam, stopping power, Bethe-formula, mean ionization potential

1 Introduction

The energy loss of ions in solids has been described with excellent theoretical background based on the theory developed by Bohr, Bethe and Bloch [1, 2, 3, 4], and improved upon by numerous empirical and semi-empirical contributions derived from ion-solid interaction data published in the last 90 years [5, 6, 7, 8, 9, 10, 11]. Interest in the quantification of energy loss of swift ions was primarily due to the needs of basic physics research, however, studies in the applied sciences gained in importance over the years. Furthermore, accurate determination of the stopping powers of organic materials has long been recognized as crucial for applications in radiation physics and, more recently, medicine and biology. Carbon, being a bio-compatible material with light mass, is one of the most studied elemental targets in ion transport experiments [12]. However, almost all published data on energy loss have been measured for graphite and amorphous carbon targets, that could be prepared as thin films, which is necessary for determination of ion energy loss by the transmission method. In the IAEA stopping power database [13] only two sets of energy loss results for protons in diamond have been reported, and no data for other ions is available. One of the main reasons for this was the inability to obtain diamond crystals thinned down so finely as required for these purposes.

Here, we present the results of energy loss of protons, in the energy range from 1.6 MeV to 6 MeV, in a diamond target – a self-supported membrane with micrometer thickness. The membrane was fabricated by thinning down a larger synthetic single-crystal

diamond sample through a combination of laser slicing, mechanical polishing and deep plasma etching. The energy loss was determined by passing the proton beams through the membrane portion of the sample and measuring the energy loss of the ions on the detector positioned behind it, using a well calibrated low-noise electronic chain. The results were compared with the most popular Monte Carlo transport code for ions, SRIM [14], as well as previously published data. In addition, the difference between the measured stopping power and theoretical values calculated from the Bethe formula was used to estimate the mean ionization potential of carbon atoms in diamond.

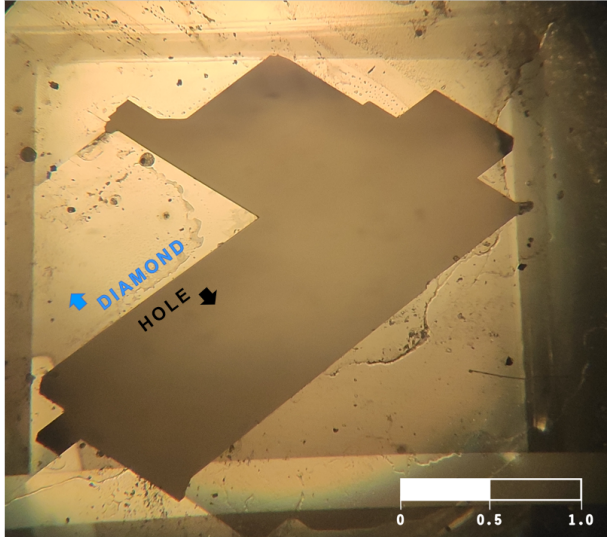
The excellent mechanical and electrical properties of diamond offer versatile potential for applications in research and industry. Technological advancements of the crystal growth process ensured wider market availability of high-purity synthetic diamond in the last 10 years. An increased interest in diamond-based devices has been reported in particle detection, outer-space electronics, medical physics, and other fields involving interaction with radiation. In recent years, progress has been made, particularly in the area of radiation microdosimeters based on diamond [15, 16]. Diamond radiation detectors have also been reported to be used in medical proton and carbon beam treatment monitoring [17, 18] and as detectors for dosimetry tests in high-rate FLASH radiotherapy [19]. Thin, self-supported diamond membranes, such as the one tested here, can also be used for radiation monitoring, after appropriate signal processing contacts are applied. Such a membrane radiation detector has already been developed and has demonstrated excellent charge collection efficiency and radiation hardness [20]. In addition, diamond membranes have also been exploited as vacuum windows for ion beam extraction into the atmosphere [21]. Beyond the listed examples, diamond is also a promising optoelectronic medium for quantum applications and single photon emitters [22, 23], where deterministic ion implantation can be used for material modification.

Transport codes are commonly used to quantify radiation-related effects in these applications, such as energy deposition per penetration length, total absorbed dose, or range of ionizing particles. The reliability of the ion transport simulations is limited for diamond due to the aforementioned problem of scarce experimental stopping cross-section data, that are used to fit the parameters of the underlying physics [24, 25]. One of the key parameters is the mean excitation potential I , a material-specific constant used in Bethe formula. The value of the mean excitation potential for carbon atoms in diamond obtained in this work is discussed and compared to previously reported I -values for graphite.

2 Materials and experimental procedure

A thin diamond crystal was used as the target material for measuring energy loss. Single-crystal chemical vapor deposited (CVD) diamond grown in $<100>$ orientation was thinned to a few micrometer thickness in a several staged process: first, the crystal was pre-thinned by laser slicing and further mechanical polishing; then, deep plasma etching was performed in the central $3 \times 3 \text{ mm}^2$ region of the crystal for the final thinning. With this procedure it was possible to prepare a diamond sample into a self-supported membrane with excellent surface quality (rms surface roughness around a few nm was measured by AFM and optical interferometry technique after the processing [26]).

Figure (1) shows under the microscope view of the diamond, where it can be seen that the central membrane region has an irregularly shaped hole. The membrane was broken as a result of the previously performed experiments. However, the sample was still perfectly usable as the target material for energy loss estimate, since the remaining diamond areas were large enough to be exposed to spatially focused ion beams, as was



Slika 1: Diamond membrane sample viewed with optical microscope. Calibration scale in bottom right corner marks 1 mm length. Irregularly shaped hole in the central portion of the membrane is visible.

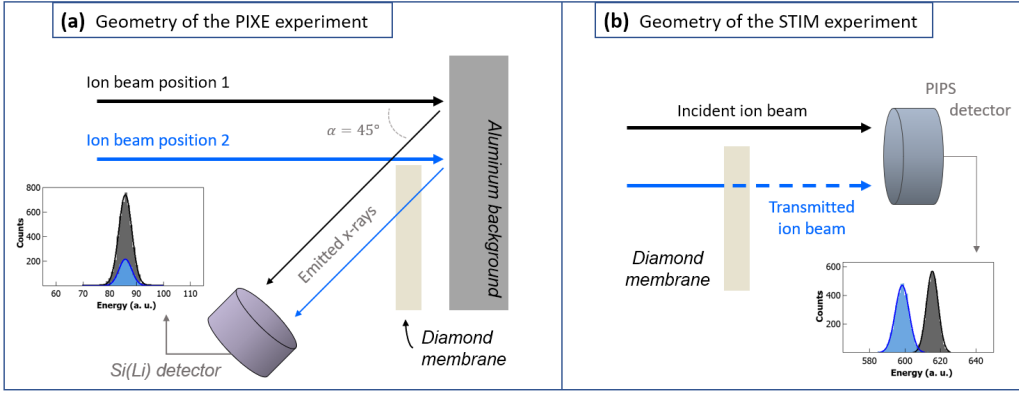
done in our experimental scenario.

In order to examine the surface quality and determine the exact thickness of the membrane, two independent methods were used: direct measurement using scanning electron microscopy (SEM) and indirect estimate from the absorption of X-rays in diamond. In SEM, focused beam of accelerated electrons was scanned over the edge of the diamond membrane, producing an image, on which the edge thickness can be directly observed and measured. For X-ray absorption, the membrane was mounted on a thick aluminum sample holder and placed in the ion microprobe vacuum chamber of the Ruđer Bošković accelerator facility [27]. Ion microprobe setup [28] allows spatial focusing of the ion beam to a micrometer-sized spot. The chamber is attached to the tandem Van de Graaff electrostatic accelerator for production of fast MeV ion beams, that were used to induce X-rays. The analysis of ion-generated X-rays is referred to as Particle Induced X-Ray Emission (PIXE) technique. The geometry of the experimental setup is schematically shown in Figure (2)-(a). A 2 MeV proton beam was used to induce X-rays in the background element made from aluminum. The beam can be scanned over the selected areas of the sample, and spatially resolved information can be obtained. The Si(Li) X-ray detector was positioned at an angle of $\alpha = 135^\circ$ relative to the beam axis. Diamond membrane is located between the background element and the detector. When the proton beam is at a position near the edge of the membrane (for example – position 2 in figure (2)-(a)), the X-rays that reach the detector are attenuated by passing through the membrane. When the beam is positioned far away from the membrane (position 1 in Figure (2)-(b)), the X-rays are not attenuated. According to the Beer-Lambert law [29], the X-ray intensity after passing a distance Δx through the absorber will be:

$$I = I_o \exp(-\mu \rho \Delta x), \quad (1)$$

where I_o is the X-ray beam intensity before attenuation, μ is the absorption coefficient and ρ is the density of the material. Δx can be evaluated from the ratio of attenuated and unattenuated X-rays. Since X-rays detected in our experiment transmit the diamond at angle α , the thickness of the membrane is calculated as $\Delta x \cos(\alpha)$.

For the measurement of the stopping power, MeV protons of different energies were passed through the membrane, and the energy loss of transmitted ions was recorded. Ion



Slika 2: Schematic view of the experiment geometry with the diamond membrane in the ion microprobe vacuum chamber for: (a) Thickness measurement using X-ray attenuation, (b) Energy loss measurement using transmission method.

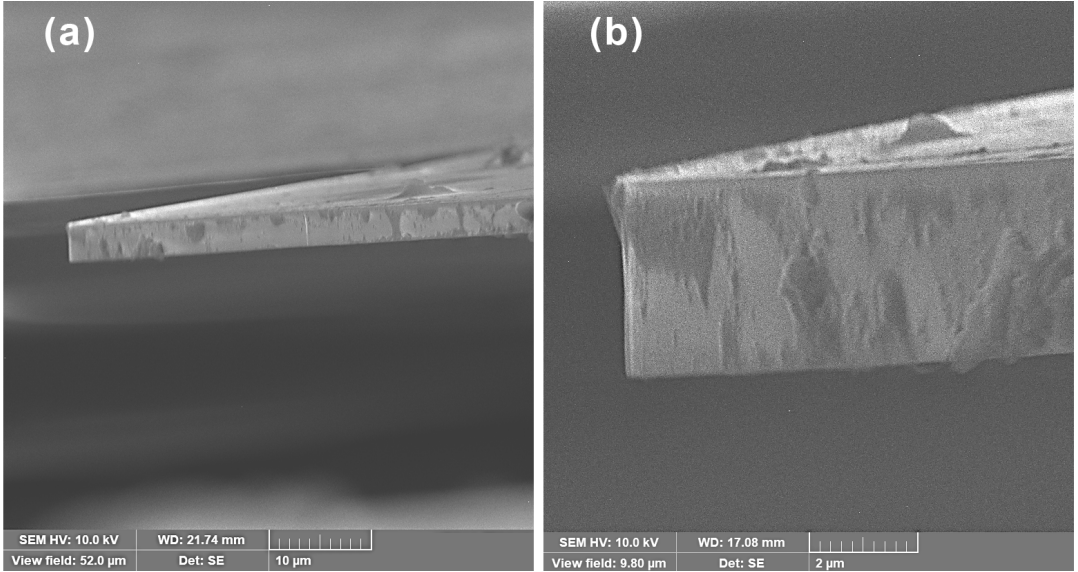
microprobe setup was again used, and the ion beam was cut by two sets of apertures used to define a beam spot by collimating action. After being accelerated, ions pass through the 90-degree magnet to ensure that the correct ion mass and energy is selected before reaching the experimental chamber. The membrane was mounted on the sample holder with a transmission window through which ions could reach a detector positioned directly in the beam axis behind the sample (as shown in Figure (2)-(b)). During the experiment, the proton beams were scanned across the desired membrane regions to record events where ions either transverse through the membrane or where they don't. This technique is sometimes referred to as scanning transmission ion microscopy (STIM) and is used to generate 2D maps of the transmitted ion energy. Beam currents were kept at the order of fA. The transmitted ions were stopped in the Passivated Implanted Planar Silicon (PIPS) detector [30], with a very thin entrance window (< 50 nm). Standard signal processing electronics, based on a charge sensitive preamplifier (ORTEC 142A) and a shaping amplifier (ORTEC 570), were used. The energy resolution of the whole electronic chain was about 40 keV for 1.6 MeV protons and 60 keV for 6 MeV protons. The energy loss was determined from the acquired pulse height spectra of the transmitted ions.

3 Results and discussion

Diamond membrane thickness

Figure (3) shows a magnified view of one of the membrane edges imaged with SEM. Membrane thickness was measured at various points along the edge using this and 5 other SEM images of different membrane regions (not shown here), resulting in an average value of (3.5 ± 0.1) μm . In the SEM scans, it can be seen that the membrane edge is not positioned perfectly perpendicular to the electron beam. This effect, in combination with the depth of field limitations, was the main source of uncertainty in reading out the membrane thickness with higher precision.

To further verify the membrane thickness, the X-ray attenuation through the diamond was measured using the PIXE technique and the scanning ion microbeam. X-ray intensity spectra were extracted from the regions-of-interest in the collected X-ray intensity maps, one corresponding to beam position 1 and the other corresponding to position 2, as explained in Figure (2)-(a). The extracted intensity spectra are also shown in the inset of the same figure. Only X-rays of the Al K_α line were counted. The intensity was



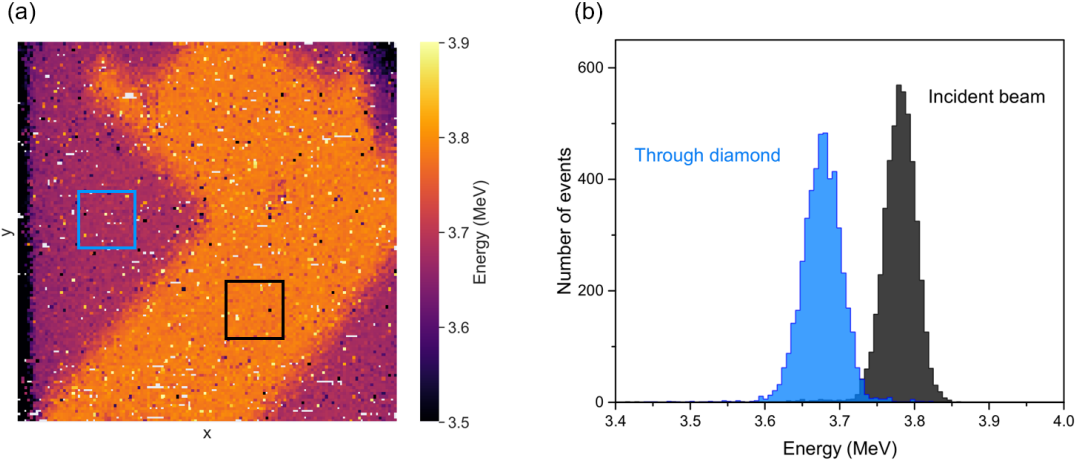
Slika 3: (a) SEM image of the portion of the diamond membrane edge, and (b) higher magnification image.

calculated as the area of the Gaussian fit to both spectra. The ratio of the two intensities was used to derive the thickness using the equation (1), with the resulting value of $\Delta x = (3.5 \pm 0.3) \mu\text{m}$. In this way, the thickness of the diamond membrane was indirectly estimated. In order to check the surface uniformity of the sample, X-ray counts were extracted from different regions of the map and the calculations were repeated, always producing the same result for the thickness. The obtained value of Δx is in excellent agreement with the thickness extracted from the SEM scans. The average of the results measured by these two methods is $(3.5 \pm 0.2) \mu\text{m}$. This mean thickness value was used in the further calculations for the experimental stopping powers, as it is the best estimate of the membrane thickness and surface homogeneity available to us due to the limitations of the used experimental methods.

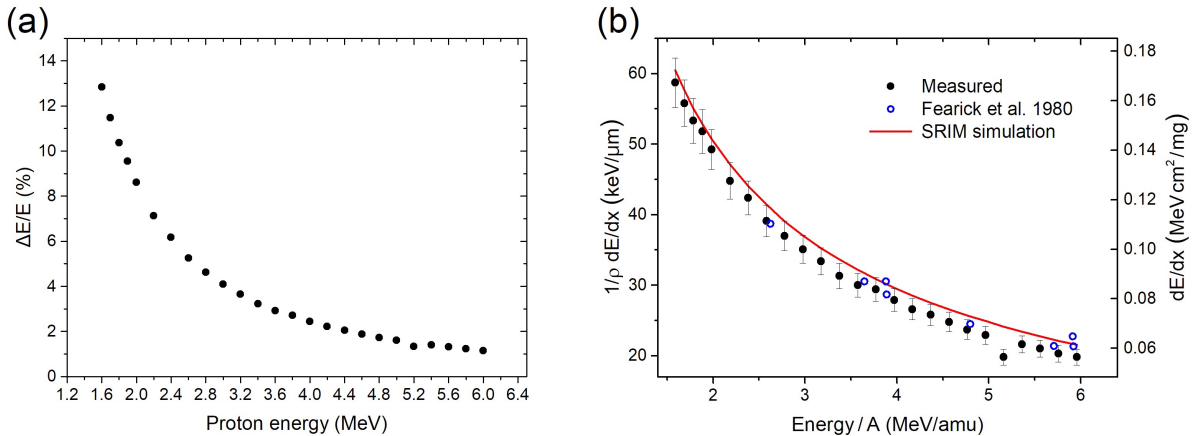
Energy loss and stopping power

The energy loss of protons with energies from 1.6 MeV to 6 MeV in diamond was measured by the transmission method using a scanning ion beam. The ion energy was increased by a step of 0.1 MeV for energies between 1.6 MeV and 2 MeV and by a step of 0.2 MeV for higher energies. Figure (4)-(a) shows one representative 2D distribution (STIM map) of the transmitted ion energy for 3.8 MeV protons. The color scale corresponds to the average collected energy in each spatial coordinate.

By comparing this map with the under the microscope view from Figure (1), one can immediately recognize the regions of the map where the ions have penetrated through the membrane (transmitted ions have lower energy). Figure (4)-(b) shows energy spectra extracted from the two regions-of-interest in this map, a diamond and a hole region. The energy distribution of the collected ions exhibits a clean peak behavior and allows us to accurately determine the energy loss of ions, ΔE , in the membrane. The energy loss data in units of $\Delta E/E$, where E is the energy of the incident ions, are plotted in Figure (5)-(a). It can be seen that the energy deposited in the membrane accounts for less than 15% of the initial ion energy over the entire energy range covered (and for all energies above 1.8 MeV - $\Delta E/E$ is less than 10%). It has already been shown that, for the energy loss of MeV protons, the equality $\Delta E/\Delta x = dE/dx$ can be assumed to be valid as long as ΔE



Slika 4: Results of ion transmission measurement (STIM) for 3.8 MeV protons. (a) 2D distribution map of energy of transmitted protons. (b) Corresponding ion energy spectra, extracted from the regions marked in the map (a).



Slika 5: Energy loss of protons in diamond: (a) Relative energy loss $\Delta E/E$ as a function of incident proton energy E . (b) Energy loss in stopping power units plotted together with the results of SRIM simulation and previously reported data [32].

does not exceed 20% of the total ion energy [31]. Therefore, measured energy loss data can be used to accurately calculate the stopping powers. The obtained values of stopping power are shown in Figure (5)-(b). The vertical axis of the plot is represented both in energy and mass stopping units. The error bars for each point were calculated to account for both the statistical treatment of the energy loss spectra and the uncertainty in the diamond thickness.

In Figure (5)-(b) we have also included the diamond stopping power data for protons reported by Fearick and Sellschop (1980) [32]. A good overall matching between two data sets can be observed. In addition, we can include the stopping powers predicted by the transport code SRIM (shown as a solid red line in the same plot) and observe that the simulated data points show a small but noticeable systematic offset to higher values compared to the experimental stopping powers reported here. At lower energies, the SRIM prediction and measured values agree within the experimental uncertainty. However, the difference becomes more pronounced with increasing proton energy: from 3% at 1.6 MeV to about 8% at 6 MeV. To calculate stopping power, SRIM relies on the parameters based on the available data of energy loss in amorphous carbon, and then performs density

correction for diamond. It can be speculated that this approximation is not adequate to fully simulate the consequences that tight atomic bonding in diamond crystal lattice has on the energy loss mechanisms [33]. Measuring the energy loss in a broader energy range and for other ion species would allow for a more comprehensive comparison of the experimental results and the SRIM simulations, and consequently for more substantial conclusions to be made.

It should also be noted that one of the measured stopping powers (for 5.2 MeV protons) deviates from the general trend of the measured data. Since there appears to be no obvious nuclear phenomenon that could affect the proton-diamond interaction at this specific energy, it is likely that the lower value was recorded due to an inadvertent experimental error. However, this should be confirmed by an independent experiment. On a general note, the energy loss of MeV proton projectiles was measured with good accuracy, determined by the already discussed sources of uncertainty, with diamond thickness estimate being the only significant one.

Mean ionization potential

The electronic stopping power of a target material with atomic number Z_2 and atomic weight $M_2(u)$, for ions with atomic number Z_1 and velocity v , can be theoretically described by the Bethe formula:

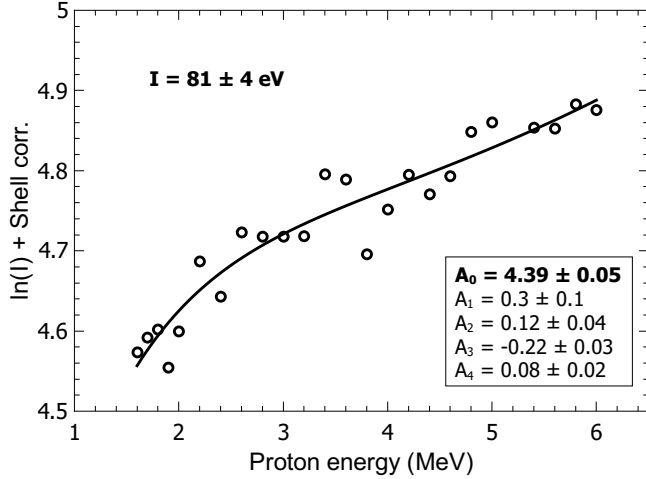
$$S = \frac{\kappa Z_2}{\beta^2} Z_1^2 \left\{ f(\beta) - \frac{C}{Z_2} - \ln(I) - \frac{\delta}{2} + Z_1 L_1 + Z_1^2 L_2^2 \right\}, \quad (2)$$

where, $f(\beta)$ is defined as:

$$f(\beta) = \ln \left[\frac{2m_e c^2 \beta^2}{1 - \beta^2} \right] - \beta^2, \quad (3)$$

and, for stopping units of keV/(mg/cm²), $\kappa = 0.3071/M_2(u)$ and $\beta = v/c$. The following contributions to the stopping power, grouped in the parenthesis, are: factor $f(\beta)$ (already defined), shell correction C/Z_2 , mean ionization potential I , density correction $\delta/2$, the Barkas-Anderson correction $Z_1 L_1$ and the Bloch correction $Z_1^2 L_2^2$.

In order to determine the mean ionization potential of carbon atoms in diamond, we compared the measured diamond stopping powers with the theoretical values. Certain approximations were used to evaluate the Bethe formula. First, Bloch and density contributions were neglected because the former should account for less than 1% of the stopping power at energies above 1 MeV/amu [34] and the latter, the density effect, is completely negligible for nonrelativistic energies of projectile ions. The Barkas-Anderson correction was determined using Ziegler's empirical formula [35], while the $f(\beta)$ contribution was calculated directly. The two remaining contributions, $C/Z_2 + \ln(I)$, are the shell correction and the mean ionization potential. The shell effect corrects for the assumption that the velocity of the ion is much higher than the velocity of the target electrons, and accounts for the ion's interaction with each of the electronic orbits. Therefore, the shell correction is a function of the ion energy. Several models have been developed to estimate this function for different materials, usually either within the formalism where the atomic electrons of the target material are described by hydrogenic wave functions (HWF), or by using the local density approximation (LDA) where the ions are assumed to interact with the free electron gas. We have avoided using any of these approaches for the calculation because they depend either on empirical parameters, that are not available for diamond, or on theoretical assumptions that may bias the results. Our approach was based on the empirical results of Ziegler and Anderson [36], who found, based on a large data set of



Slika 6: Estimate of the mean ionization potential: extracted values of $C/Z_2 + \ln(I)$ (circles) have been fitted to the function (4). Fitting result is plotted as a solid line, while the parameters of the approximation are given in the inset of the graph.

proton stopping in 27 different target materials, that the energy dependence of the shell correction can be well approximated with the following power series:

$$\frac{C}{Z_2} = A_0 + A_1 \ln(E) + A_2 [\ln(E)]^2 + A_3 [\ln(E)]^3 + A_4 [\ln(E)]^4 , \quad (4)$$

and in this equation, parameter $A_0 = \ln(I)$. Therefore, we extracted the combined contributions of the shell correction and the mean ionization potential from the difference between the measured stopping powers and the described Bethe theory, giving us:

$$\frac{C}{Z_2} + \ln(I) = f(\beta) + Z_1 L_1 - \frac{S_{\text{exp}} \beta^2}{\kappa Z_1^2 Z_2} , \quad (5)$$

and fitted these values to the equation (4) to evaluate the ionization energy I .

Figure (6) shows the $\ln(I) +$ Shell correction contributions to the diamond stopping power, extracted from the data according to the equation (5), as well as the results of the fitting according to the equation (4). Mean ionization potential is calculated as $I = 81 \pm 4$ eV. Other parameters of the polynomial fit to the experimental data are listed in the inset of the graph.

In 2016, the International Commission on Radiation Units and Measurements (ICRU) recommended the use of the I -value of 81 eV for graphite, based on the results of M.S. MacPherson [37]. The previously recommended value was 78 eV [38]. Other estimates for the mean ionization energy of carbon atoms in graphite were also reported close to the value of 80 eV (Bichsel and Tschalar [39] and Sakamoto et al. [40]). It should be noted that the evaluation of the I -value in the papers published by different groups is influenced by the underlying assumptions used in the modelling of the stopping power. Since diamond is an allotropic form of carbon with strong atomic bonding and tightly-packed crystal structure, it may have a different excitation energy, expected to be somewhat higher than that of graphite [25]. In a recent paper, Fernández-Varea et al. [41] estimated the I -value for diamond to be 88.5 eV, based on electron and positron stopping power data. However, the mean ionization potential calculated here is consistent with the previously reported results for graphite. Our approach was limited mainly by the fact that the exploited empirical model (4) is a nonlinear 4-parameter equation fitted to a data set with relatively

large statistical variance. In the context of the available literature, where the estimates of I -values have also been obtained indirectly from comparison of experimental stopping powers and theoretical models, it is reasonable to surmise that the mean ionization potential of 81 eV for diamond, reported here, is a relevant result of potential use for the community.

4 Conclusions

In summary, energy losses of MeV protons, transmitted through a thin diamond membrane, were measured in the energy range from 1.6 to 6 MeV. The thickness and surface uniformity of the diamond target were quantified both through direct (SEM) and indirect (PIXE) imaging techniques. An ion microprobe setup was used for energy loss experiments in which the membrane was exposed to focused proton beams that were scanned over the sample to easily extract energy loss of those ions that were transmitted in the forward direction through the membrane. The obtained stopping powers are in the close agreement with those calculated by the transport code SRIM, but, with a systematic offset to lower stopping power values. Also, by comparing experimental and theoretical stopping powers, we calculated the mean ionization potential of carbon atoms in diamond. I -value of 81 eV was extracted, which agrees with the before published results for graphite.

These experimental data are valuable because previous results of ion energy loss in diamond are extremely scarce. This limits the efforts to systematically quantify the electronic and nuclear energy loss of ions in diamond crystals, information that is crucial for simulating ion transport based on Bethe's theory as well as other empirical and semi-empirical models. The presented results are hoped to be useful for further experimental and theoretical studies of radiation interactions with diamond, which are needed to improve precision of calculations such as energy deposition or absorbed radiation dose, resulting with a more reliable use of this material in cutting-edge technologies for medical dosimetry, particle tracking etc. Obtaining even thinner diamond membranes would enable extending energy loss measurements for lower ion energies and heavier ions.

Literatura

- [1] N. Bohr. II. *On the theory of the decrease of velocity of moving electrified particles on passing through matter. The London, Edinburgh, and Dublin Philosophical Magazine and Journal of Science*, 25(145):10–31, January 1913.
- [2] N. Bohr. LX. *On the decrease of velocity of swiftly moving electrified particles in passing through matter. The London, Edinburgh, and Dublin Philosophical Magazine and Journal of Science*, 30(178):581–612, October 1915.
- [3] H. Bethe. Bremsformel für Elektronen relativistischer Geschwindigkeit. *Zeitschrift für Physik*, 76(5-6):293–299, May 1932.
- [4] F. Bloch. Bremsvermögen von Atomen mit mehreren Elektronen. *Zeitschrift für Physik*, 81(5-6):363–376, May 1933.
- [5] U Fano. Penetration of Protons, Alpha Particles, and Mesons. *Annual Review of Nuclear Science*, 13(1):1–66, December 1963.

- [6] Hans Henrik Andersen and J. F. Ziegler. *Hydrogen stopping powers and ranges in all elements*. Number v. 3 in The Stopping and ranges of ions in matter. Pergamon Press, New York, 1977.
- [7] Mitio Inokuti. Inelastic Collisions of Fast Charged Particles with Atoms and Molecules—The Bethe Theory Revisited. *Reviews of Modern Physics*, 43(3):297–347, July 1971.
- [8] Peter Sigmund. Kinetic theory of particle stopping in a medium with internal motion. *Physical Review A*, 26(5):2497–2517, November 1982.
- [9] James F. Ziegler and Jochen P. Biersack. The Stopping and Range of Ions in Matter. In D. Allan Bromley, editor, *Treatise on Heavy-Ion Science*, pages 93–129. Springer US, Boston, MA, 1985.
- [10] L. H. Andersen, P. Hvelplund, H. Knudsen, S. P. Möller, J. O. P. Pedersen, E. Uggerhøj, K. Elsener, and E. Morenzoni. Measurement of the Z 1 3 contribution to the stopping power using MeV protons and antiprotons: The Barkas effect. *Physical Review Letters*, 62(15):1731–1734, April 1989.
- [11] Jens Lindhard and Allan H. So/rensen. Relativistic theory of stopping for heavy ions. *Physical Review A*, 53(4):2443–2456, April 1996.
- [12] D.I. Thwaites. Review of stopping powers in organic materials. *Nuclear Instruments and Methods in Physics Research Section B: Beam Interactions with Materials and Atoms*, 27(2):293–300, June 1987.
- [13] Electronic Stopping Power of Matter for Ions.
- [14] James F. Ziegler, M.D. Ziegler, and J.P. Biersack. SRIM – The stopping and range of ions in matter (2010). *Nuclear Instruments and Methods in Physics Research Section B: Beam Interactions with Materials and Atoms*, 268(11-12):1818–1823, June 2010.
- [15] Izabella A. Zahradník, Michal T. Pomorski, Ludovic De Marzi, Dominique Tromson, Philippe Barberet, Natko Skukan, Philippe Bergonzo, Guillaume Devès, Joël Herault, Wataru Kada, Thierry Pourcher, and Samuel Saada. scCVD Diamond Membrane based Microdosimeter for Hadron Therapy. *physica status solidi (a)*, 215(22):1800383, November 2018.
- [16] C. Verona, G. Magrin, P. Solevi, M. Bandorf, M. Marinelli, M. Stock, and G. Verona Rinati. Toward the use of single crystal diamond based detector for ion-beam therapy microdosimetry. *Radiation Measurements*, 110:25–31, March 2018.
- [17] A. K. Mandapaka, A. Ghebremedhin, B. Patyal, Marco Marinelli, G. Prestopino, C. Verona, and G. Verona-Rinati. Evaluation of the dosimetric properties of a synthetic single crystal diamond detector in high energy clinical proton beams: Dosimetry of synthetic diamond detector in proton beams. *Medical Physics*, 40(12):121702, November 2013.
- [18] Séverine Rossomme, Marco Marinelli, Gianluca Verona-Rinati, Francesco Romano, Pablo Antonio Giuseppe Cirrone, Andrzej Kacperek, Stefaan Vynckier, and Hugo Palmans. Response of synthetic diamond detectors in proton, carbon, and oxygen ion beams. *Medical Physics*, 44(10):5445–5449, October 2017.

- [19] Annalisa Patriarca, Charles Fouillade, Michel Auger, Frédéric Martin, Frédéric Pouzoulet, Catherine Nauraye, Sophie Heinrich, Vincent Favaudon, Samuel Meyroneinc, Rémi Dendale, Alejandro Mazal, Philip Poortmans, Pierre Verrelle, and Ludovic De Marzi. Experimental set-up for flash proton irradiation of small animals using a clinical system. *International Journal of Radiation Oncology*Biology*Physics*, 102(3):619–626, 2018.
- [20] N. Skukan, I. Sudić, M. Pomorski, W. Kada, and M. Jakšić. Enhanced radiation hardness and signal recovery in thin diamond detectors. *AIP Advances*, 9(2):025027, February 2019.
- [21] V. Grilj, N. Skukan, M. Pomorski, W. Kada, N. Iwamoto, T. Kamiya, T. Ohshima, and M. Jakšić. An ultra-thin diamond membrane as a transmission particle detector and vacuum window for external microbeams. *Applied Physics Letters*, 103(24):243106, December 2013.
- [22] J Achard, V Jacques, and A Tallaire. Chemical vapour deposition diamond single crystals with nitrogen-vacancy centres: a review of material synthesis and technology for quantum sensing applications. *Journal of Physics D: Applied Physics*, 53(31):313001, July 2020.
- [23] Carlo Bradac, Weibo Gao, Jacopo Forneris, Matthew E. Trusheim, and Igor Aharonovich. Quantum nanophotonics with group IV defects in diamond. *Nature Communications*, 10(1):5625, December 2019.
- [24] Vaiva Kaveckyte, Åsa Carlsson Tedgren, and José M Fernández-Varea. Impact of the i-value of diamond on the energy deposition in different beam qualities. *Physics in Medicine & Biology*, 66(12):125004, jun 2021.
- [25] Pedro Andreo and Hamza Benmakhlof. Role of the density, density effect and mean excitation energy in solid-state detectors for small photon fields. *Physics in Medicine and Biology*, 62(4):1518–1532, jan 2017.
- [26] Michal Pomorski, Benoit Caylar, and Philippe Bergonzo. Super-thin single crystal diamond membrane radiation detectors. *Applied Physics Letters*, 103(11):112106, September 2013.
- [27] Iva Bogdanović Radović. Ruder Bošković Institute Accelerator Facility. *Nuclear Physics News*, 30(2):4–9, April 2020.
- [28] M. Jakšić, I. Bogdanović Radović, M. Bogovac, V. Desnica, S. Fazinić, M. Karlušić, Z. Medunić, H. Muto, Ž. Pastuović, Z. Siketić, N. Skukan, and T. Tadić. New capabilities of the Zagreb ion microbeam system. *Nuclear Instruments and Methods in Physics Research Section B: Beam Interactions with Materials and Atoms*, 260(1):114–118, July 2007.
- [29] Thomas G. Mayerhöfer, Susanne Pahlow, and Jürgen Popp. The Bouguer-Beer-Lambert Law: Shining Light on the Obscure. *ChemPhysChem*, 21(18):2029–2046, September 2020.
- [30] PIPS® Detectors Passivated Implanted Planar Silicon Detectors.
- [31] H.H. Andersen, A.F. Garfinkel, C.C. Hanke, and H. Sørensen. Stopping power of aluminium for 5-12 mev protons and deuterons. *Det Kongelige Danske Videnskabernes Selskab, Matematisk-Fysiske Meddelelser*, 35(4):24 pp., 1966.

- [32] R.W. Fearick and J.P.F. Sellschop. Energy loss of light ions in diamond. *Nuclear Instruments and Methods*, 168(1-3):51–55, January 1980.
- [33] W. Käferböck, W Rössler, V. Necas, P. Bauer, M. Peñalba, E. Zarate, and A. Arnau. Comparative study of the stopping power of graphite and diamond. *Phys. Rev. B*, 55:13275–13278, May 1997.
- [34] Martin Berger, M Inokuti, H Andersen, H Bichsel, D Powers, Stephen Seltzer, D Thwaites, and D Watt. Stopping powers for protons and alpha particles, 1993-01-01 1993.
- [35] James F. Ziegler, Jochen Biersack, and Matthias D. Ziegler. *SRIM - the stopping and range of ions in matter*. SRIM, Chester, Maryland, 2015.
- [36] Hans Henrik Andersen and J. F. Ziegler. *Hydrogen stopping powers and ranges in all elements*. Number v. 3 in The Stopping and ranges of ions in matter. Pergamon Press, New York, 1977.
- [37] Miller Macpherson. *Accurate measurements of the collision stopping powers for 5 to 30 MEV electrons*. Doctor of Philosophy, Carleton University, Ottawa, Ontario, 1998.
- [38] International Commission on Radiation Units and Measurements, editor. *Stopping powers for electrons and positrons*. Number 37 in ICRU report. International Commission on Radiation Units and Measurements, Bethesda, Md., U.S.A, 1984.
- [39] H Bichsel and C Tschalär. Range difference measurements for protons in c, al, sapphire, si, quartz, ge, and ag. *Bull. Am. Phys. Soc.*, 10:723, 1965.
- [40] N. Sakamoto, H. Ogawa, and N. Shiomi-Tsuda. Stopping powers of carbon for protons from 4 to 13 MeV. *Nuclear Instruments and Methods in Physics Research Section B: Beam Interactions with Materials and Atoms*, 115(1-4):84–87, July 1996.
- [41] José M Fernández-Varea, Bartosz Górká, and Bo Nilsson. Electronic stopping power of diamond for electrons and positrons. *Physics in Medicine & Biology*, 66(16):165003, August 2021.